

Supramolecular Solar Cells: Surface Modification of Nanocrystalline TiO₂ with Coordinating Ligands To Immobilize Sensitizers and Dyads via Metal–Ligand Coordination for Enhanced Photocurrent Generation

Navaneetha K. Subbaiyan, Channa A. Wijesinghe, and Francis D'Souza*

Department of Chemistry, Wichita State University, 1845 Fairmount, Wichita, Kansas 67260-0051

Received August 7, 2009; E-mail: Francis.DSouza@wichita.edu

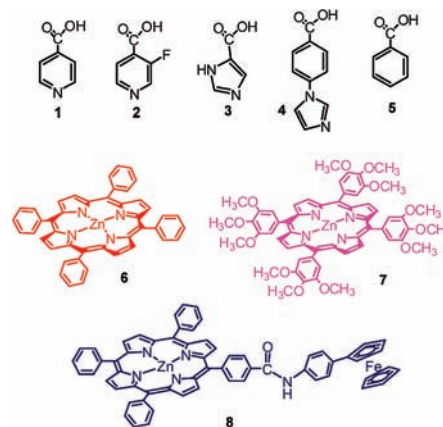
In nature, self-assembly through noncovalent binding motifs,^{1a} such as hydrogen bonding, metal–ligand coordination, and electrostatic, π - π , and weak van der Waals interactions, plays a dominant role. For example, photosynthetic antenna reaction center pigments use such intermolecular forces to precisely arrange the donor–acceptor entities in a protein matrix, exhibiting a cascade of vectorial energy and electron transfer processes.^{1b,c} Inspired by this revelation, several groups have constructed supramolecular photosynthetic architectures to mimic the photoinduced energy and electron transfer processes, with an ultimate goal of building efficient light-energy-harvesting devices based on these biomimetic principles.^{2,3} Solar cells based on biomimetic principles could serve as an alternative to semiconductor-based ones for renewable energy production. Here, the design and construction of electron- and hole-transporting nanostructured architectures are pivotal for enhancing both charge separation efficiency and charge carrier mobility to improve the photovoltaic response.³ Although donor–acceptor-type dyads have frequently been utilized for this purpose,² examples employing noncovalent methodologies, especially the highly versatile metal–ligand binding approach⁴ for assembling the different entities on the electrode surface, have been scarce.⁵

Here we report a metal–ligand axial coordination approach⁴ for the assembly of zinc tetrapyrrole sensitizers as well as a (donor)₁–(donor)₂ type dyad instead of the frequently used donor–acceptor-type dyads² on semiconducting TiO₂ surfaces. As demonstrated here, the present approach not only allows testing of the photoelectrochemical behavior of different zinc tetrapyrroles but also enables us to utilize fairly complex structures involving more than one donor entity. Additionally, utilization of the dyad markedly improves the current–voltage (*I*–*V*) performance of the photoelectrochemical cell through an electron transfer–hole migration mechanism.

In a typical experiment, a thin noncrystalline TiO₂ film-coated F-doped tin oxide (FTO) electrode (~10–12 μ m, tec7 from Pilkington) was surface-modified with an axially coordinating ligand bearing a carboxylic acid (compounds 1–5 in Chart 1) by placing the electrode in an ethanolic solution of the desired compound overnight. After removal of the unbound molecules (two or three ethanol washings), the TiO₂ electrode was immersed in an *o*-dichlorobenzene (DCB) solution containing the desired zinc tetrapyrrole (6–8 in Chart 1) for 20–30 min. After this, the electrodes were rinsed with DCB to remove excess uncoordinated zinc

via axial coordination of the zinc tetrapyrroles^{4,5} in the case of TiO₂ surfaces modified with 1–4.

Chart 1. Structures of the Nitrogenous Ligands Possessing Carboxylic Acids Used To Modify the TiO₂ Surface (1–4), the Sensitizers (6 and 7), and the Dyad (8) Used To Axially Coordinate the Immobilized Nitrogenous Bases on the TiO₂ Surface; 5 is a Control Compound Lacking the Axial Ligand Entity



Photoelectrochemical cells were constructed using platinumized indium tin oxide as the counter electrode in noncoordinating DCB

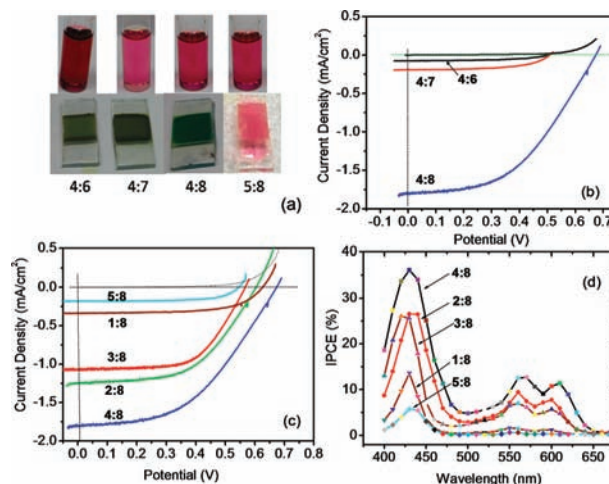
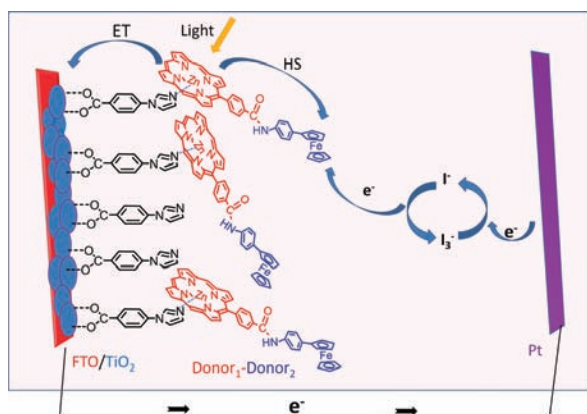


Figure 1. (a) Pictures of sensitizers in solution and on the FTO–TiO₂ electrodes modified with 4 or 5. (b) *I*–*V* characteristics showing the effect of different sensitizers bound to 4-modified TiO₂. (c) *I*–*V* characteristics showing the effect of different surface modifiers on the photoelectrochemical behavior upon binding of 8. (d) IPCE curves for the electrodes used in (c). The *I*–*V* curves were generated in DCB containing I₃[−]/I[−] (0.5 M/0.03 M) redox mediator using an AM 1.5 simulated light source with a 340 nm UV cutoff filter. The black lines in (b) and (c) are dark currents recorded for the 4:8-modified electrode.

containing 0.5 M (*n*-Bu)₄NI and 0.03 M I₂ as the redox mediator (see the SI for experimental details). We chose four nitrogenous bases with different p*K*_a values⁶ to modify the TiO₂ surface, two zinc tetrapyrroles (**6** and **7**) having slightly different spectral and redox behaviors to demonstrate the versatility of the present method, and a zinc porphyrin–ferrocene (ZnP–Fc) (donor)₁–(donor)₂-type dyad (**8**) to exhibit improved photoelectrochemical behavior as a result of an electron transfer–hole migration mechanism.

Figure 1b shows typical *I*–*V* plots for sensitizers bound to **4**-modified TiO₂. Similar-looking *I*–*V* plots with lower photocurrents were obtained for electrodes modified with surface modifiers **1**–**3**. The photocurrents (*I*_{SC}) generated for **4:6**- and **4:7**-modified electrodes were nearly an order of magnitude smaller than that obtained for the dyad **4:8**-modified electrode. The photovoltages (*V*_{OC}) were also found to be smaller for the former electrodes. For the **4:8**-modified electrode, the *V*_{OC} and *I*_{SC} were found to be 0.67 V and 1.6 mA/cm², respectively. Furthermore, the performance of this dyad was tested for other surface modifiers. As shown in Figure 1c, higher currents were obtained for each of these electrodes than for those modified with simple sensitizers. For a given zinc tetrapyrrole, the *I*–*V* performance for the various surface modifiers followed the order **4** > **2** > **3** > **1** > **5**, that is, it largely followed the metal–ligand binding constants of a given zinc tetrapyrrole.⁶ The incident-photon-to-current efficiency (IPCE) plots for the electrodes used in Figure 1c are shown in Figure 1d. The shapes resembled those of the absorbance spectra of the sensitizers (see Figures S1 and S3 in the SI for the UV–vis spectra and IPCE curves, respectively, for the other sensitizer electrodes), suggesting that they are indeed responsible for the photovoltaic behavior. Additionally, photoswitching experiments revealed reproducible photocurrent generation (Figure S4 in the SI), indicating little or no dissociation of the coordinated sensitizer. The IPCEs at the Soret band locations were found to be 37, 28, 26, 14, and 6%, respectively, for the electrodes with **4:8**-, **2:8**-, **3:8**-, **1:8**-, and **5:8**-modified surfaces. For the **4:8**-modified photocell, the fill-factor and conversion efficiencies were found to be 47% and 0.56, respectively.

Scheme 1. Schematics of the Zinc Porphyrin–Ferrocene Dyad (**8**) Surface Modified via Axial Coordination of **4** Immobilized onto the TiO₂ Film on the FTO Electrode (the Photochemical and Redox Processes Are Shown by Arrows)



The photochemical events resulting in enhanced photocurrent in the case of the ZnP–Fc (donor)₁–(donor)₂ dyad-modified TiO₂ electrode are shown in Scheme 1. Excitation of the donor zinc porphyrin of the dyad results in injection of an electron into TiO₂, generating ZnP^{•+}.⁷ Because of favorable redox potentials,⁸ a hole migration subsequently occurs, neutralizing ZnP^{•+} and resulting in

the formation of Fc⁺. The mediator I[–] neutralizes Fc⁺ to form I₃[–], which is subsequently reduced by the photoejected electron via the counter electrode, thus closing the circuit. The present electron transfer–hole migration mechanism¹⁰ differs from the sequential electron transfer (from the photoexcited donor to the acceptor to the TiO₂) often observed in the case of donor–acceptor-modified electrodes,² signifying the importance of the present biomimetic approach for superior photovoltaic performance.

In summary, we have devised an elegant method of self-assembly for modification of a TiO₂ surface using coordinating ligands followed by immobilization of variety of sensitizers and a dyad. A maximum IPCE value of 37% was achieved for the TiO₂ electrode modified with **4:8**, a novel feature that is attributed to an electron transfer–hole migration mechanism of the dyad. Currently, utilization of this approach to modify nanocrystalline TiO₂ and other semiconductor surfaces using different (donor)₁–(donor)₂, donor–acceptor, and antenna-donor-type dyads and triads and evaluation of their photoelectrochemical performance and the kinetics of electron ejection and hole migration are in progress in our laboratory.

Acknowledgment. This work was financially supported by the National Science Foundation (Grant 0804015) and NSF-EPSCoR grants.

Supporting Information Available: Experimental details, UV–vis spectra of the investigated sensitizers in solution and on the TiO₂/FTO surface, IPCE curves, and light switching of photocurrent generation. This material is available free of charge via the Internet at <http://pubs.acs.org>.

References

- (1) (a) Lehn, J.-M. *Supramolecular Chemistry: Concepts and Perspectives*; VCH: Weinheim, Germany, 1995. (b) Deisenhofer, J.; Epp, O.; Miki, K.; Huber, R.; Michel, H. *Nature* **1986**, *318*, 618. (c) Renger, G. *Primary Processes of Photosynthesis: Principles and Apparatus*; RSC Publishing: Cambridge, U.K., 2008.
- (2) (a) Imahori, H.; Umeyama, T.; Ito, S. *Acc. Chem. Res.* **2009**, ASAP Article (DOI: 10.1021/ar900034t). (b) Günes, S.; Neugebauer, H.; Sariciftci, N. S. *Chem. Rev.* **2007**, *107*, 1324. (c) Segura, J. L.; Martin, N.; Guldi, D. M. *Chem. Soc. Rev.* **2005**, *34*, 31. (d) Thompson, B. C.; Fréchet, J. M. J. *Angew. Chem., Int. Ed.* **2008**, *47*, 58. (e) Kamat, P. V. *J. Phys. Chem. C* **2007**, *111*, 2834. (f) Fukuzumi, S. *Phys. Chem. Chem. Phys.* **2008**, *10*, 2283. (g) Balzani, V.; Credi, A.; Venturi, M. *ChemSusChem* **2008**, *1*, 26. (i) Imahori, H.; Fukuzumi, F. *Adv. Funct. Mater.* **2004**, *14*, 525.
- (3) (a) *Organic Nanostructures for Next-Generation Devices*; Atwood, J. L., Steed, J. W., Eds.; Springer-Verlag: Berlin, 2008. (b) Grätzel, M.; Durrant, J. R. In *Series on Photoconversion of Solar Energy*; Archer, M. D., Nozik, A. J., Eds.; World Scientific: Singapore, 2009; Vol. 3, pp 503–538. (c) Goncalves, L. M.; de Zea Bermudez, V.; Ribeiro, H. A.; Mendes, A. M. *Energy Environ. Sci.* **2008**, *1*, 655. (d) *Organic Photovoltaics: Device Physics and Manufacturing Technologies*; Brabec, C. J., Dyakonov, V., Scherf, U., Eds.; Wiley-VCH: Weinheim, Germany, 2009.
- (4) (a) Carvino, A.; Sariciftci, N. S. *J. Mater. Chem.* **2002**, *12*, 1931. (b) Kira, A.; Umeyama, T.; Matano, Y.; Yoshida, K.; Isoda, S.; Park, J. K.; Kim, D.; Imahori, H. *J. Am. Chem. Soc.* **2009**, *131*, 3198. (c) Fischer, M. K. R.; Lopez-Duarte, I.; Wienk, M. M.; Martinez-Diaz, M. V.; Janssen, R. A. J.; Bäuerle, P.; Torres, T. *J. Am. Chem. Soc.* **2009**, *131*, 8669. (d) Subbaiyan, N. K.; Obratsov, I.; Wijesinghe, C. A.; Tran, K.; Kutner, W.; D'Souza, F. *J. Phys. Chem. C* **2009**, *113*, 8982.
- (5) (a) D'Souza, F.; Ito, O. *Coord. Chem. Rev.* **2005**, *249*, 1410. (b) Chitta, R.; D'Souza, F. *J. Mater. Chem.* **2008**, *18*, 1440.
- (6) D'Souza, F.; Deviprasad, G. R.; Zandler, M. E.; Hoang, V. T.; Klykov, A.; Perera, M.; van Stipdonk, M. J.; El-Khouly, M. E.; Fujitsuka, M.; Ito, O. *J. Phys. Chem. A* **2002**, *106*, 3243.
- (7) Photoinduced electron transfer from ¹ZnP* to Fc in **8** occurs at a rate of 6.0 × 10⁸ s^{–1} (see ref 9), suggesting that the electron injection from ¹ZnP* to TiO₂ is faster than this process.
- (8) The first oxidation of ZnP in **8** is located at 0.31 V while that of Fc is located at 0.0 V vs Fc/Fc⁺ in DCB (see ref 9).
- (9) D'Souza, F.; Smith, P. M.; Gadde, S.; McCarty, A. L.; Kullman, M. J.; Zandler, M. E.; Ito, M.; Araki, Y.; Ito, O. *J. Phys. Chem. B* **2004**, *108*, 11333.
- (10) Kleverlaan, C.; Alebbi, M.; Argazzi, R.; Bignozzi, C. A.; Hasselmann, G. M.; Meyer, G. J. *Inorg. Chem.* **2000**, *39*, 1342.

JA9067113